THE LINAC COHERENT LIGHT SOURCE AT SLAC*

P. Emma

Stanford Linear Accelerator Center, Stanford, California 94309, USA

Abstract

A design study [1] has been completed at SLAC for a linac-based Free Electron Laser (FEL) known as the Linac Coherent Light Source (LCLS), which aims at the production of high peak power coherent x-rays with a wavelength of 1.5 Å. A 1-nC electron beam produces coherent radiation through self-amplified spontaneous emission (SASE) in a long undulator with a projected peak output power of ~10 GW. The design utilizes the last kilometer of the SLAC linac, not used by the PEP-II project, to compress and accelerate a single electron bunch, generated by a photocathode rf gun, to a peak current of ~3.4 kA at 15 GeV. We describe here the acceleration, compression and preservation of this high brightness electron beam through the S-band linac and related transport lines, and outline some of the required beamline modifications. Specific challenges such as emittance growth generated by coherent synchrotron radiation, compensation of the correlated electron energy spread after compression, and overall pulse-to-pulse machine stability issues drive the parameter choices and system designs outlined here.

1 INTRODUCTION

The LCLS is based on the principle of Self-Amplified-Spontaneous-Emission (SASE) where high power, transversely coherent, radiation is generated in a single pass of a high peak current electron beam through a long undulator eliminating the need for optical cavities, which are difficult to build in the x-ray spectral region.

The requirements on the electron beam are, however, quite demanding and, until recently, difficult to achieve. The LCLS will utilize the experience and technical advances gained at the Stanford Linear Collider (SLC) [2] and the Final Focus Test Beam (FFTB) [3] and make use of recent progress in the production of intense electron beams with radio-frequency photocathode guns [4].

With the advent of the PEP-II asymmetric B-factory, which employs only the first 2/3 of the 3-km SLAC linac, the final kilometer will be available to accelerate and compress an electron beam up to 17 GeV. With these developments, as well as ongoing studies for the next linear collider (NLC) [5], SLAC is in an ideal position to construct a linac based x-ray FEL. This was first proposed in 1992 [6]. This new '4th generation' source will produce

coherent radiation many orders of magnitude greater in peak power and brightness than present 3rd generation sources, opening new research potentials in chemistry, physics, biology and other applied sciences. The main parameters, at the undulator, are outlined in Table 1.

Table 1: LCLS parameters at 15 and 1.5 Å operation.

Parameter	unit	15 Å	1.5 Å
Electron beam energy	GeV	4.54	14.35
Repetition rate	Hz	120	120
Normalized emittance†	μm	2.0	1.5
Peak beam current	kA	3.4	3.4
Coherent energy spread†	%	<0.2	<0.1
Incoherent energy spread†	%	<0.06	<0.02
Bunch length†	μm	20	20
Beam size†	μm	37	31
Field gain length	m	3.7	11.7
Undulator period	mm	30	30
FEL parameter	10^{-4}	12.9	4.7
Peak brightness	$10^{32\,\ddagger}$	1.2	12
Average brightness	$10^{22\,\ddagger}$	0.42	4.2
Peak saturation power	GW	11	9
Peak spontaneous power	GW	8.1	81

† RMS,   ‡ photons/sec/mm^2/mrad^2/0.1%-BW

Table 1 shows parameters at the low and high energy ends of the operational range, with radiation wavelengths of 15 and 1.5 Å, respectively. The 100-m, permanent magnet, planar undulator will be located in the existing FFTB tunnel, directly following the linac. The accelerator is divided into several sections to provide two-stage bunch compression. A schematic layout of the accelerator is shown in Fig. 1 which includes the RF-gun (at the 2-km point in the linac), four linac sections (Linac-0…3), two dog-leg transport lines (DL1,2) two bunch compressors (BC1,2) and the undulator. System parameters and electron beam quantities are indicated at various points.
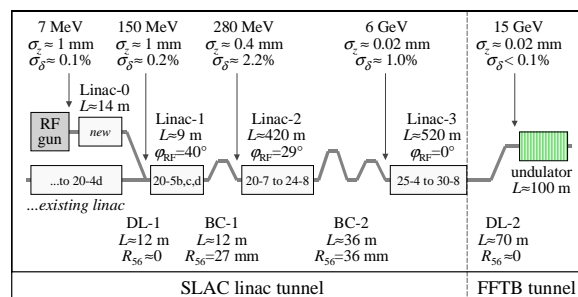
**Fig. 1**: LCLS accelerator and compressor schematic.

The first linac (Linac-0) is a new section installed adjacent to the existing linac which accelerates the 1 mm

---

long bunch to 150 MeV and also compensates the space charge induced transverse emittance growth. The first bend section (DL1) injects the beam into the main linac and provides emittance and energy spread diagnostics. Linac-1 (L1) accelerates the 1 mm bunch 'off-crest' to 280 MeV and generates an energy correlation along the bunch such that the first chicane bunch compressor (BC1) shortens the bunch to 0.38 mm. L2 then accelerates the bunch to 6 GeV and also generates an energy correlation so the double chicane system (BC2) compresses the bunch to its design value of 20 μm. Finally, L3 nominally accelerates the beam to 15 GeV (a range of 4-17 GeV is available) and also cancels the remaining correlated energy spread with its geometric wakefield. The high-energy dog leg (DL2) is designed for energy and energy spread analysis, transverse emittance measurements, final beam transport, and variable matching into the undulator.

All of the linac sections, except L0, are existing and require only minor modifications. Both L2 and L3 (~950 meters of linac) require primarily quadrupole power supply modifications, while L1 (9 meters) requires the insertion of a few quadrupole magnets. The bunch compressors and DL1 will be composed of some new and some existing magnet designs and replace a total of 15 3-meter rf structures (4 klystrons) for an energy loss of ~2% of the nominal 50 GeV SLAC linac. DL2 and the post-undulator electron beam dump will use the existing FFTB tunnel as well as its magnets.

The peak current required for 1.5-Å SASE saturation in the 100-m undulator is dependent on the final emittance as shown in Fig. 2. Plotted is the 'slice' emittance, defined as the transverse phase space area over of a small slice (~0.5 μm) of the 20 μm bunch length. Conversely, the whole-bunch emittance, 'projected' emittance, may be significantly larger, with little impact on saturation. The LCLS design budgets a 50% slice emittance increase over the entire accelerator. Considering most dilution mechanisms affect the projected emittance, rather than the slice, this is a relatively conservative budget.
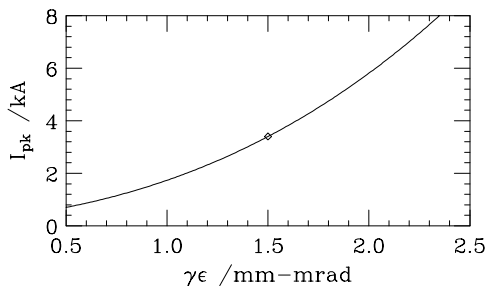
Fig. 2: Peak current required for 1.5 Å SASE saturation in the 100-m undulator vs. rms normalized 'slice' emittance.

2 LONGITUDINAL DYNAMICS

To achieve the high peak current in the undulator, the bunch must be compressed in a series of magnetic chicanes. These will be arranged and located along the linac such that non-linearities in the compression and acceleration process (wakefields, rf curvature, and 2nd order momentum compaction) are mutually canceled. With a careful arrangement the compression process is more linear which reduces the minimum bunch length achievable. An optimum choice of parameters cancels the final correlated energy spread, minimizes transverse emittance growth effects and desensitizes the system to phase and charge variations.

2.1 Bunch Compression

The bunch is compressed by accelerating at an off-crest rf phase, thereby introducing a correlated energy spread along the bunch. This is followed by a bending section, a magnetic chicane, with linear path length dependence on particle energy. The peak current generated by the rf photocathode gun is ~100 Amps. Generating the 3.4 kA necessary for 1.5-Å SASE saturation at $\gamma\varepsilon = 1.5 \mu$m requires a compression factor of ~35. For a single stage compressor using an rf phase of φ_0, the relative change in final bunch length, $\Delta\sigma_f/\sigma_f$, produced by a change in initial beam phase, $\Delta\varphi$, (timing jitter at the gun) is given by [7]

$$\frac{\Delta\sigma_f}{\sigma_f} \approx -\left(\frac{\sigma_i}{\sigma_f} \mp 1\right)\Delta\varphi \cot\varphi_0 , \qquad (1)$$

with 'under-compression' ($<\pi/2$ phase space rotation) expressed by the minus sign and 'over-compression' the plus sign. For $\varphi_0 = 20°$ and a compression factor of $\sigma_i/\sigma_f = 35$, initial phase jitter of just $\Delta\varphi = 0.1°$ S-band (0.1 psec) results in final bunch length (undulator peak current) jitter of $\Delta\sigma_f/\sigma_f \approx 16\%$.

Clearly, a single stage compressor is too sensitive. Furthermore, the final bunch length of a single stage compressor is limited by non-linearities, such as rf curvature, which make single-stage compression from 1 mm to 20 μm very difficult. A two-stage compression system, however, brings about cancellations which can reduce this phase jitter sensitivity by an order of magnitude. This also allows the first compressor to be located early in the accelerator so that the next linac section accelerates a shorter bunch. The reduced transverse wakefield of the shorter bunch provides looser quadrupole and rf-structure alignment tolerances. Conversely, a single compression stage needs to be placed at a high enough energy so that space charge forces are not significant for a 20 μm bunch. This extends the length over which the long bunch is accelerated tightening alignment tolerances. For these reasons, a two-stage compressor is used.

The compressors are simple 4-dipole chicanes with no quadrupoles. These offer ease of adjustment and the dispersion function is closed to all orders in energy.

The first compressor (BC1) is at 280 MeV and shortens the bunch from 1 mm to 385 μm rms at a correlated energy spread of 2.2% rms. The second compressor (BC2) is a double chicane designed to reduce and

compensate the transverse emittance growth generated by coherent synchrotron radiation (CSR) [8] (explained below). BC2 is at 6 GeV and compresses the bunch from 385 μm to ~20 μm rms at a correlated energy spread of 1.0% rms. Bunch length diagnostics, using e.g. CSR [9], are included after each bend section. Table 2 summarizes the chicanes.

Table 2: Bunch compressor chicane parameters.

| Parameter	unit	BC1	BC2 chic-1	BC2 chic-2
Beam energy	GeV	0.28	6	6
Total length	m	2.8	13.2	13.2
Momentum compac.	mm	27	31	4.5
Dipole length	m	0.2	1.5	1.5
Bend angle/dipole	deg	7.1	3.4	1.3
Drift between bends	m	0.75	3.35	3.35
Max. dispersion	m	0.12	0.29	0.11

Fig. 3 shows a simulation of longitudinal phase space before and after each compressor. The non-linear correlation after BC1 (Fig. 3b) is primarily due to the long bunch on the S-band rf curvature in L1. It is later compensated by the geometric wakefield of L2 resulting in the nearly linear correlation of Fig. 3c. Finally, after BC2, the large correlated energy spread (Fig. 3d) is cancelled by acceleration and the strong geometric wakefield of the L3 linac (see Fig. 4, lower right).
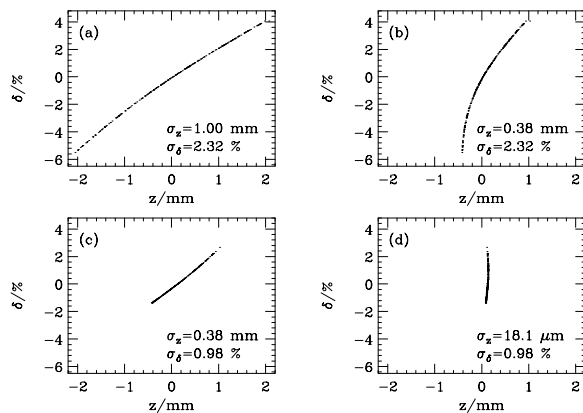
Fig. 3: Longitudinal phase space on fixed scales at (a) BC1-start, (b) BC1-end, (c) BC2-start and (d) BC2-end (bunch head at left).

The core of the beam (85%) is shown, prior to the undulator, in Fig. 4. The final energy spread is 0.035% rms with a very acceptable incoherent component (over a 0.5 μm slice) of 0.006%. Large energy tails (~1%) which encompass 15% of the bunch charge are not shown. The simulations [10] include geometric wakefields, the sinusoidal character of the rf accelerating field, the 1st and 2nd order momentum compaction of the chicanes, and the incoherent energy spread generated by synchrotron radiation in BC2 and DL2. The resistive wall wakefields of L3/DL2 and CSR effects of BC2/DL2 are not included in the figures, and are expected to contribute <0.05% rms

to the coherent energy spread, some of which is correctable through small adjustments in the rf phasing.
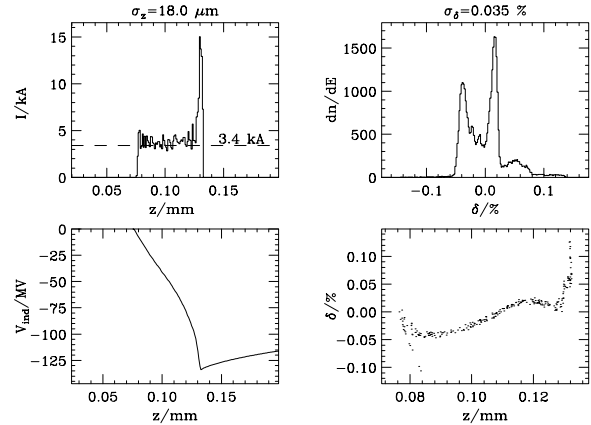
Fig. 4: Longitudinal phase space (low-right), axial (up-left) and energy (up-right) distributions and L3 bunch induced voltage (low-left) at undulator input (15 GeV).

The chosen chicane locations, the intermediate bunch length, and the rf phases form a system with significantly looser tolerances on pulse-to-pulse gun jitter. Gun timing jitter of 0.8 psec rms or initial bunch population jitter of 3% rms will each produce a 10% rms peak current jitter. Although challenging, they are achievable.

2.2 Coherent Synchrotron Radiation

When a microbunch follows a curved path, as in a chicane, the bunch radiates at wavelengths which may be large compared to the bunch length. This coherent radiation produces an energy-spread-generating wakefield along the bunch which can induce significant transverse emittance growth; a potential problem for many future microbunch accelerators.

In the LCLS, this is controlled by using a double chicane [11] for the 2nd bunch compressor. Chicane-1 of the double system is designed to partially compress the bunch, keeping the emittance growth due to incoherent synchrotron radiation less than 2%. A second chicane is then added with reduced bend angles and separating optics (four quadrupoles forming a $-\mathbf{I}$ transfer matrix) to complete the compression and approximately cancel the net CSR emittance increase. Fig. 5 shows a schematic.
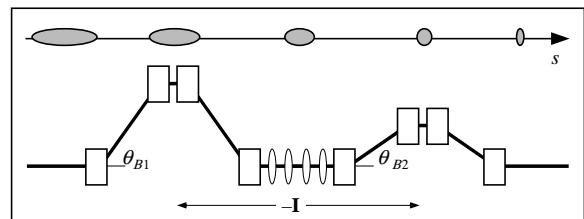

Fig. 5: Schematic of the double chicane compressor.

The cancellation can be understood by imagining an electron which loses energy in the nth dipole ($n = 1...4$) of chicane-1. In this steady-state model, the CSR-wakefield

increases with compression, but its shape along the bunch, is preserved through the chicane. The electron will then receive an extra horizontal kick, with respect to an on-energy electron, in the nth bend. This same electron, with its unchanged relative axial position, will lose even more energy in the nth bend of chicane-2 (because of the shorter bunch there), but due to the $-\mathbf{I}$ transfer matrix between paired bends and the weaker bends of chicane-2, the net horizontal kick is zero. This assumes the electron does not shift axially with respect to the remainder of the bunch as would occur in the case of over-compression or a highly non-linear phase space transformation. The double chicane also significantly weakens the CSR effect by using strong bends when the bunch is long (chicane-1) and weak bends where the bunch is short (chicane-2).

Calculations of the CSR-induced emittance dilution have been made using both a simple steady-state model and also the DESY *WAKE* code [12] which includes CSR field transients and bend-to-bend coupling effects. These calculations predict an emittance growth after BC2 of 0.3% and 3-5%, respectively. Fig. 6 shows the dispersion, bunch length, and the CSR induced energy spread and emittance growth through the BC2 double chicane for the steady-state model. CSR effects in DL2 are similarly controlled with a ~1% emittance growth expected.
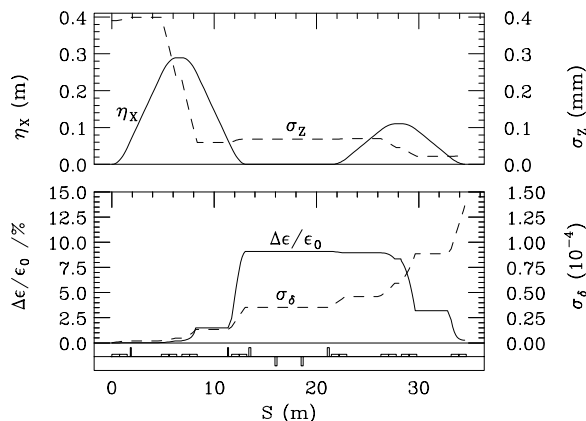
Fig. 6: The dispersion (η_x), bunch length (σ_z), and the CSR rms energy spread (σ_δ) and emittance growth ($\Delta\varepsilon/\varepsilon_0$), generated in BC2 calculated with the steady-state model.

3 TRANSVERSE DYNAMICS

The four separate S-band linac sections each have different beam parameters which motivate different lattice parameter choices. The lattices are designed to minimize 'projected' emittance dilution due to wakefields and dispersion which are generated through component misalignments. For example, a large beam energy spread and short bunch length require weak focusing.

3.1 RF Gun and Booster Linac

The high brightness electron beam is initially generated in a 1.6-cell S-band rf photocathode gun driven by a $500\,\mu$J UV laser system with temporal pulse shaping

capability and <1 psec stability. The injector is required to produce a single electron bunch of 1-nC and 100 A peak current at a repetition rate of 120 Hz with normalized rms emittances of $1\,\mu$m. The gun design includes a solenoidal field, located near the copper cathode, which initiates a compensation of the space charge induced transverse emittance growth. The L0 booster linac completes the compensation and provides acceleration to 150 MeV. L0 is a new beamline constructed parallel to the existing linac and is displaced 1 meter horizontally. It includes four 3-meter rf-structures and no quadrupole magnets. Following L0 is an adjustable optical matching section and an emittance diagnostic section. The first dog leg, DL1, provides energy diagnostics and bends the beam onto the main linac axis (L1). The existing 3-meter rf-structure there is removed to provide space for injection.

3.2 Linac-1

L1 initiates the compression process by accelerating off crest, thereby generating the necessary energy-z correlation so the first chicane, BC1, will compress the bunch. L1 is composed of three existing 3-meter rf-structures. Because of the large rf phase angle and the long bunch, the rms energy spread in L1 rapidly increases from 0.2 to 2.2%. Therefore, both dispersion and transverse wakefields are potential emittance dilution mechanisms. Space charge forces here are insignificant.

The quadrupole spacing and strength requirements were determined by simulating several different lattice schemes using the computer code *LIAR* [13]. This computer program calculates the transverse emittance dilution induced along a linac by wakefields and dispersion via random quadrupole, BPM (beam position monitor), and rf-structure misalignments. It also provides various steering algorithms and empirical emittance correction techniques. With $300\,\mu$m rms quadrupole, BPM, and rf-structure transverse misalignments and one quadrupole added after each 3-meter structure, the optimum phase advance per cell is found to be near 75°. The expected emittance dilution over L1 is then ~5%.

3.3 Linac-2

The energy spread is large (1-2%) over the entire 430-meter length of L2, and the bunch is only partially compressed making L2 the most problematic linac section for emittance preservation. The lattice choice for L2 was made, as for L1, using *LIAR*, including misalignments, and varying the phase advance per cell and quadrupole spacing. By increasing the density of quadrupoles, the expected emittance dilution can be reduced, but the gains do not clearly justify the additional costs. Therefore, the existing quadrupoles are used in their present locations with an optimum phase advance of ~70°/cell. Fig. 7 shows the dilution versus phase advance per cell after 'one-to-one' steering for the existing quadrupole spacing. Note, only the 'projected' emittance is affected here.
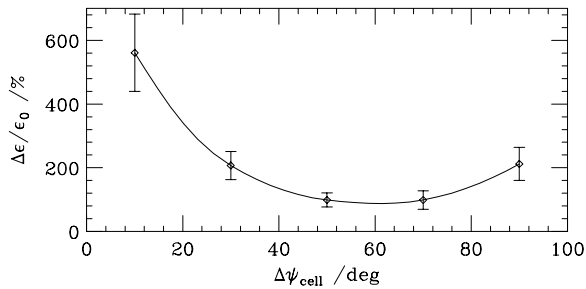
Fig. 7: Emittance after L2 vs. phase advance/cell. Quad, BPM and structure misalignments of 150,150 and 300 μm rms, respectively, and steering are applied (10 seeds).

Even though the L2 uncorrected emittance growth can easily reach 100%, localized trajectory oscillations ('bumps'), as used in the SLC and FFTB, can be applied to restore the emittance. Simulations of trajectory-based emittance corrections are performed using *LIAR*. 'Bumps' of ~300 meters in length, with 100-300 μm peak amplitude, are used to empirically minimize the measured emittance in both planes. Beam position and angle, per plane, are varied near the beginning of L2 to optimize emittances at the end. As at the SLC, oscillations are terminated with an orbit controlling feedback system. A high resolution 4-wire-scanner emittance diagnostic section is planned for the end of L2. Fig. 8 shows emittance bump correction simulations. Using 100 misalignment seeds, an average projected emittance growth of ~100% is corrected to <10% in both planes. At the FFTB, with the SLAC linac, this technique has been used to preserve an initial vertical emittance of 1.5 μm to ~50% dilution [7] while accelerating a 1-nC, 0.5-mm *long* bunch over a linac three times the length of the LCLS.
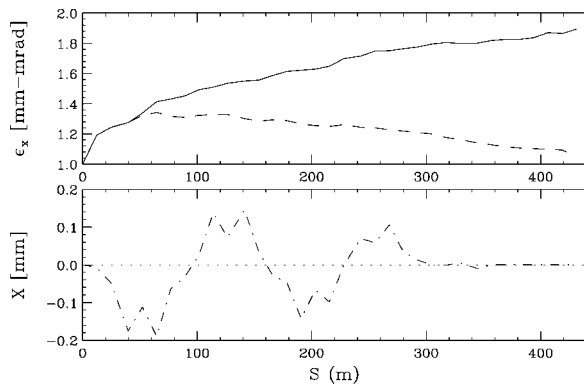
Fig. 8: Emittance along L2 before (top-solid) and after (top-dash) bumps applied. Curves are an average over 100 seeds. The bottom plot shows a typical oscillation.

3.4 Linac-3

The short bunch of L3 effectively eliminates transverse wakefields, and the rms energy spread shrinks from 1% to <0.1% due to acceleration and the strong longitudinal wakefield of the short bunch. In this case the dominant emittance dilution mechanism is due to dispersion generated by quadrupole and BPM misalignments. The

dispersion can be minimized by a weak focusing lattice. *LIAR* simulations were run for L3 using the existing linac quadrupoles and varying the phase advance per cell. In this case an optimum was found at ~30°/cell with an expected emittance dilution of <10%. A 4-wire-scanner diagnostic section presently exists at the end of L3. Finally, DL2 will include high resolution energy, energy spread and emittance diagnostics prior to the undulator.

4 SUMMARY

The LCLS offers a unique opportunity for the creation of a coherent x-ray beam with unprecedented gains in peak power and brightness using, for the most part, existing components, techniques and facilities at SLAC. Although the design is based on a consistent and feasible set of parameters, some components, such as the RF-gun, undulator construction and CSR compensation, require further research and development to guarantee performance. The present proposal includes a 3 year R&D phase with pre-fabrication engineering beginning in FY2001, construction in 2002 and major systems commissioning starting in 2005.

5 REFERENCES

[1] LCLS Design Study Report, SLAC-R-521, (1998).

[2] SLC Design Report, SLAC-PUB, (1984).

[3] FFTB Design Report, SLAC-REP-376, 1990.

[4] R.L. Sheffield, "Photocathode rf guns", *Physics of Particle Acc.*, *AIP* Vol. 184, pp. 1500-1531, (1992).

[5] Zeroth-order Design Report for the Next Linear Collider, SLAC-REP-474, May 1996.

[6] C. Pellegrini, *Workshop on Fourth Generation Light Sources,* SSRL Report 92/02, pp. 364-375, 1992.

[7] T. Raubenheimer, Nuclear Instruments and Methods in Physics Research A, 358 (1995), 40-43.

[8] See for example, Ya. S. Derbenev et al, "Microbunch Radiative Tail-Head Interaction", *DESY,* Sep. 1995.

[9] D.X. Wang, "Electron Beam Instrumentation Techniques Using Coherent Radiation*", PAC*, Vancouver, B.C., 1997.

[10] Simulations performed with the computer code *LiTrack*, written by K.L.F. Bane (SLAC).

[11] P. Emma, R. Brinkmann, "Emittance Dilution Through Coherent Energy Spread Generation in Bending Systems", *PAC*, Vancouver, B.C., 1997.

[12] M. Dohlus, T. Limberg, "Emittance Growth due to Wake Fields on Curved Bunch Trajectories", *XVIII International Free Electron Laser Conference* (Rome, 1996); DESY print *TESLA-FEL 96-13*.

[13] R. Assmann et al., "*LIAR* - A New Program for the Modeling and Simulation of Linear Accelerators with High Gradients and Small Emittances", *18th Linac Conference*, Geneva, Switzerland, August, 1996.